Electronic Supplementary Material (ESI) for Nanoscale Advances.

Support information

Te-induced fabrications of $Pt_3PdTe_{0.2}$ alloy nanocages by self-diffusion of Pd atoms with unique MOR electrocatalytic performance

Yuhe Shi,[†,a] Ling Zhang,[†,*,a] Huiwen Zhou,[a] Ruanshan Liu,[a] Shichen Nie,[b] Guojie Ye,[c] Fengxia Wu,[d,e] Wenxin Niu,[*,d,e] Jing Long Han,[*,f,g] and Ai Jie Wang[f,g]

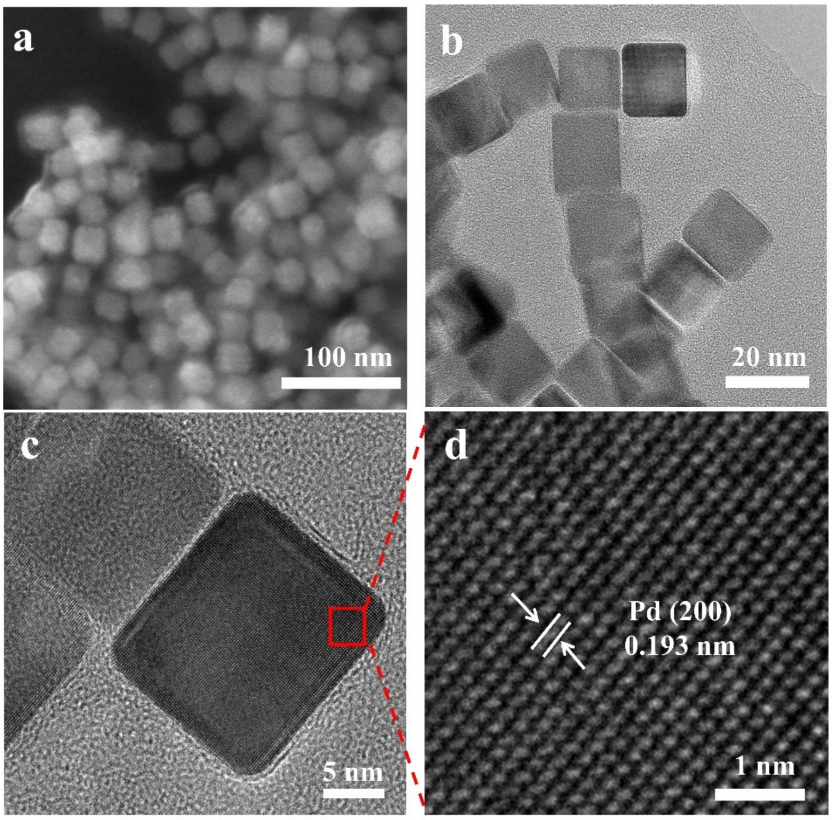

Fig. S1 SEM (a), TEM (b), and HRTEM (c and d) images of Pd nanocube templates.

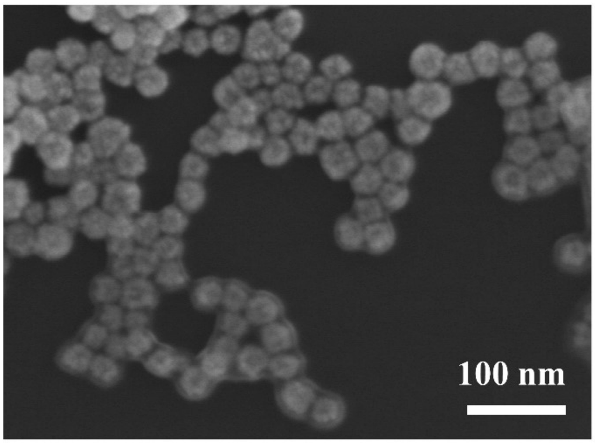

Fig. S2 SEM image of $Pt_3PdTe_{0.2}$ nanocages.

Table S1 Components ($mg \cdot L^{-1}$) of Pt, Pd, and Te elements of Pt_3PdTe_x as-products in synthetic solutions calculated from ICP-OES data.

As-products	Pt	Pd	Te
		$mg \cdot L^{-1}$	
$Pt_3PdTe_{0.2}$	16.9	3.0	0.84
$Pt_3PdTe_{0.35}$	14.8	2.7	1.1
$Pt_3PdTe_{0.4}$	15.2	2.5	1.2
Pd@Pt	4.3	2.8	–
$PtPd_{1.5}$	10.7	7.9	–

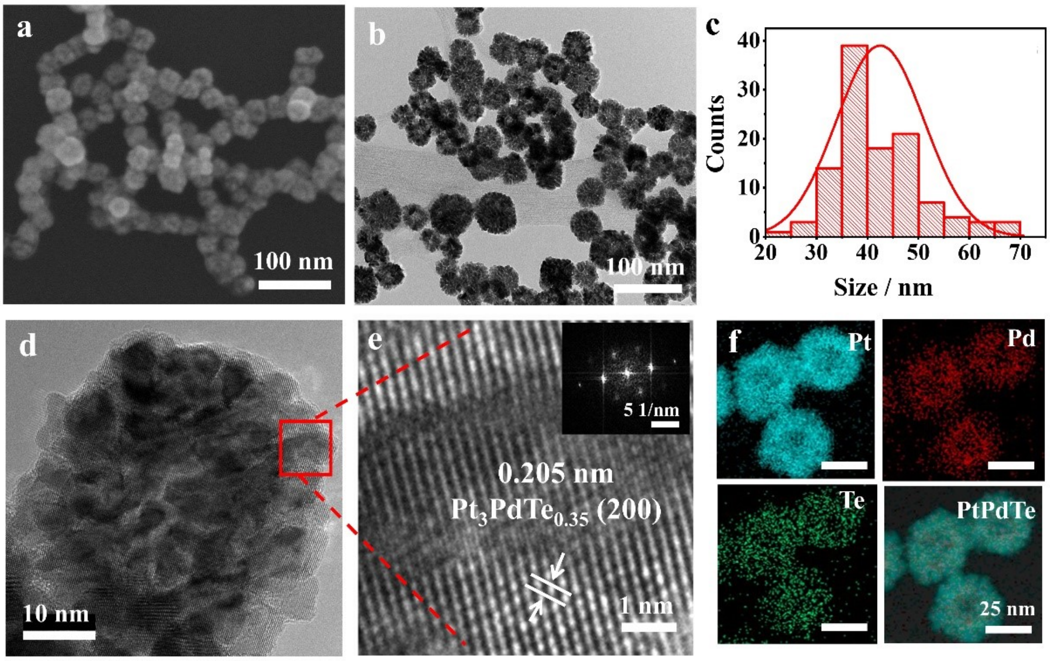

Fig. S3 SEM image (a), TEM image (b), size distribution (c), HRTEM images (d and e), and EDS elemental mappings (f) of $Pt_3PdTe_{0.35}$ nanocages. Inset of (e), corresponding FFT pattern.

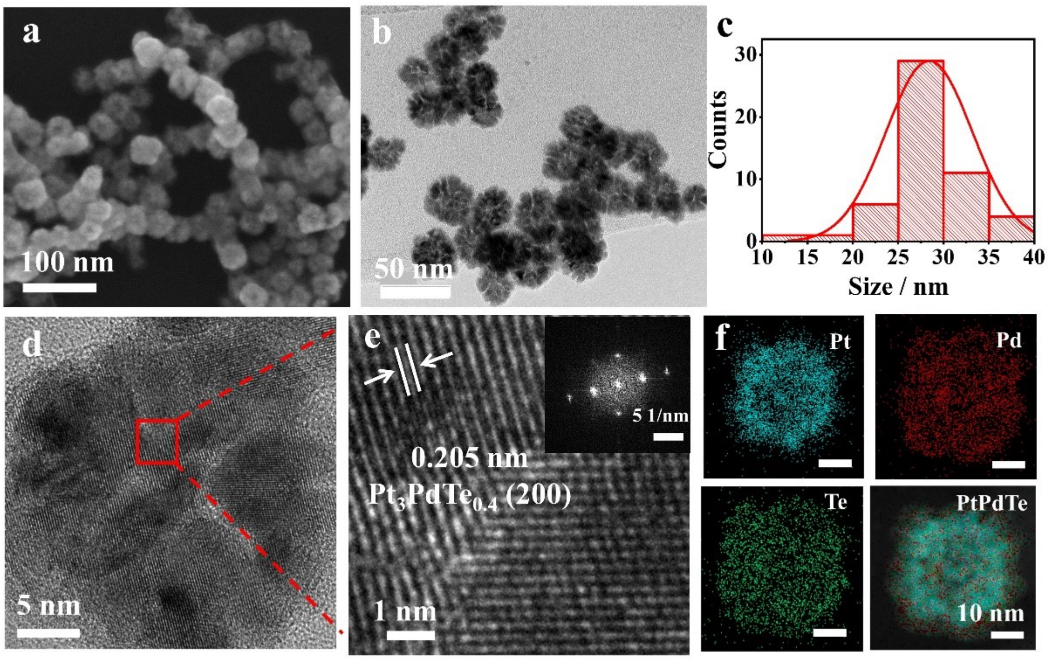

Fig. S4 SEM image (a), TEM image (b), size distribution (c), HRTEM images (d and e), and EDS elemental mappings (f) of $Pt_3PdTe_{0.4}$ nanocages. Inset of (e), corresponding FFT pattern.

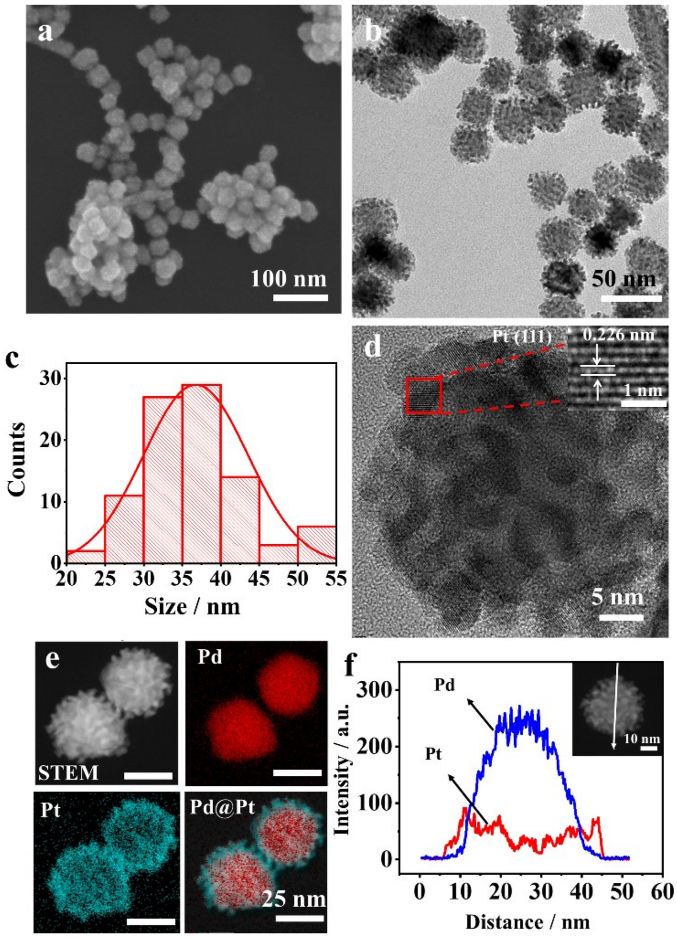

Fig. S5 SEM image (a), TEM image (b), size distribution (c), HRTEM image (d), STEM and EDS elemental mapping images (e) of Pd@Pt core-shell nanoparticles. Inset of (d), HRTEM of the labeled zone in (d). (f) Elemental linear-scan profile across the white arrow of the individual Pd@Pt core-shell nanoparticle (inset).

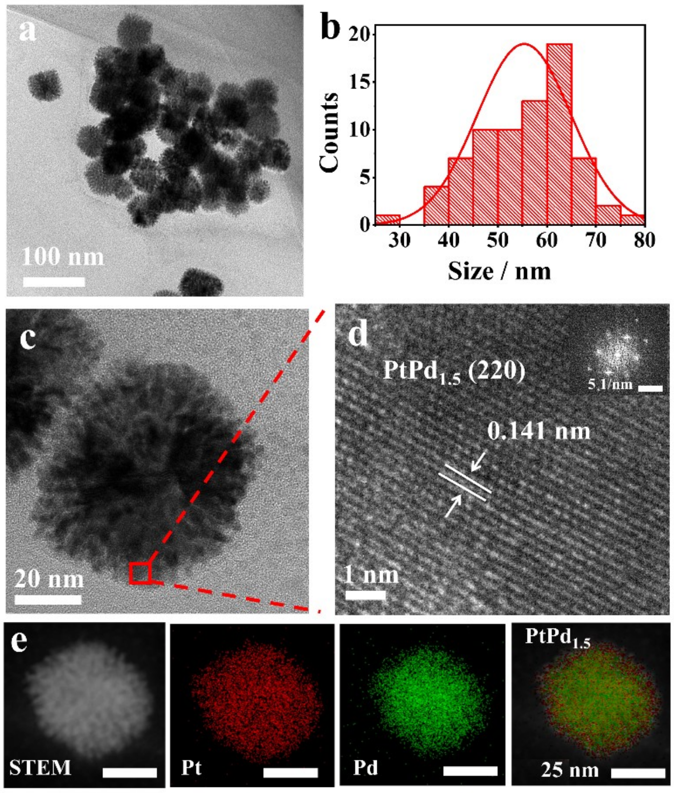

Fig. S6 TEM image (a), size distribution (b), HRTEM images (c and d), STEM and EDS elemental mapping images (e) of $PtPd_{1.5}$ alloy nanoparticles. Inset of (d), corresponding FFT pattern.

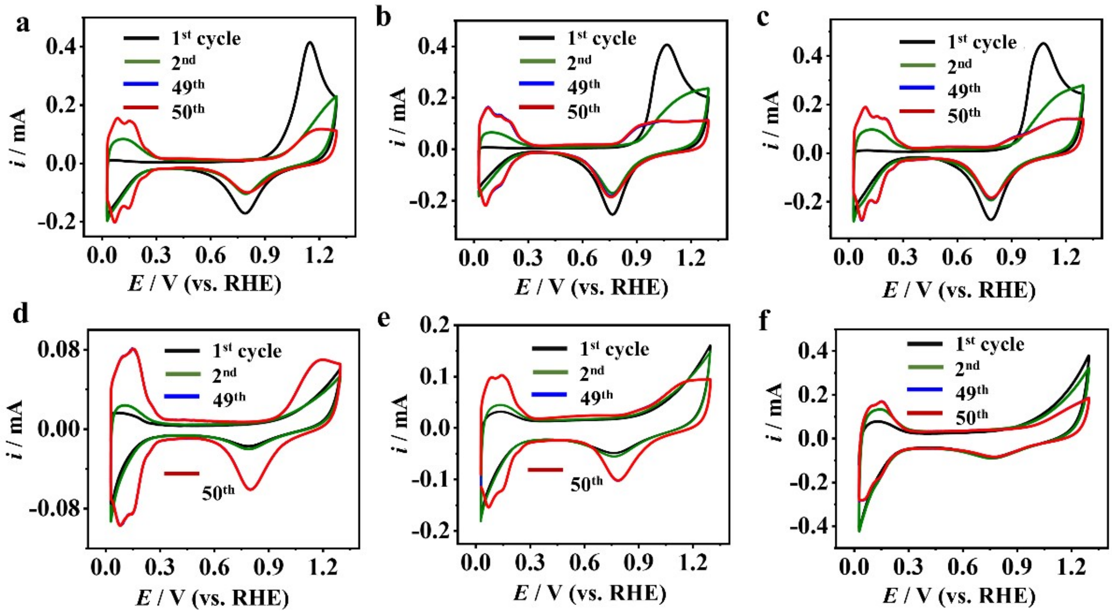

Fig. S7 CVs of $Pt_3PdTe_{0.2}$ (a), $Pt_3PdTe_{0.35}$ (b), $Pt_3PdTe_{0.4}$ (c), $PtPd_{1.5}$ (d), Pd@Pt (e), and Pt/C (f) catalysts modified GCE at 1st, 2rd, 49th, and 50th cycles in 0.5 M H_2SO_4. Scanning rates, 50 $mV{\cdot}s^{-1}$.

Table S2 Weight percentages (%) of Pt, Pd, and Te elements of Pt_3PdTe_x as-products before and after the electrochemical activations and MOR durability tests in H_2SO_4 by TEM-EDS methods.

as-products	Before activations			After activations			After durability		
	Pt	Pd	Te	Pt	Pd	Te	Pt	Pd	Te
$Pt_3PdTe_{0.2}$	92.17	4.79	3.04	90.45	8.78	0.78	90.44	8.78	0.79
$Pt_3PdTe_{0.35}$	88.37	7.14	4.54	89.26	9.6	1.18	–	–	–
$Pt_3PdTe_{0.4}$	70.65	12.23	17.12	77.12	17.27	5.63	–	–	–

Table S3. Maximum specific activities and mass activities of in the backward (j_b) and forward scan (j_f) and the ratio of j_b to j_f (I_b/I_f).

catalysts	j_b		j_f		I_b/I_f
	$mA \cdot cm^{-2}$	$A \cdot mg^{-1}$	$mA \cdot cm^{-2}$	$A \cdot mg^{-1}$	
$Pt_3PdTe_{0.2}$	2.71	2.14	1.96	1.42	1.4
$Pt_3PdTe_{0.35}$	2.36	1.85	1.57	1.13	1.5
$Pt_3PdTe_{0.4}$	1.65	0.98	1.25	0.71	1.3
Pd@Pt	1.11	0.91	0.92	0.74	1.2
$PtPd_{1.5}$	0.58	0.16	0.54	0.15	1.1
Pt/C	0.24	0.18	0.25	0.20	0.95

Table S4. Summary of reported catalytic performance of various Pt-based MOR catalysts in acidic electrolytes.

Catalysts	Electrolyte	Mass activity ($A \cdot mg^{-1}_{Pt+Pd}$)	Specific activity ($mA \cdot cm^{-2}$)	Ref.
$Pt_3PdTe_{0.2}$	0.1 M $HClO_4$, 1 M CH_3OH	2.14	2.71	This work
PdPtRuTe nanotubes	0.5 M H_2SO_4, 1.0 M CH_3OH	1.262	2.96	1
PtPdTe nanowires	1 M CH_3OH, 0.5 M H_2SO_4	–	1.49	2
PtTe nanotubes	0.5 M H_2SO_4, 0.5 M CH_3OH	0.632	1.149	3
TePbPt nanotube	0.5 M H_2SO_4, 1 M CH_3OH	0.53	–	4
PtIrTe nanotubes	0.5 M H_2SO_4, 1.0 M CH_3OH	0.495	–	5
PdRuPt nanowires	0.1 M $HClO_4$, 0.5 M CH_3OH	1.10	1.98	6
PtRu nanowires	0.1 M $HClO_4$, 0.5 M CH_3OH	0.82	1.16	7
hollow Pt-on-Pd nanodendrites	0.5 M H_2SO_4, 1.0 M CH_3OH	0.58	1.36	8
PtPdCu	0.5 M H_2SO_4, 0.5 M CH_3OH	0.52	0.693	9

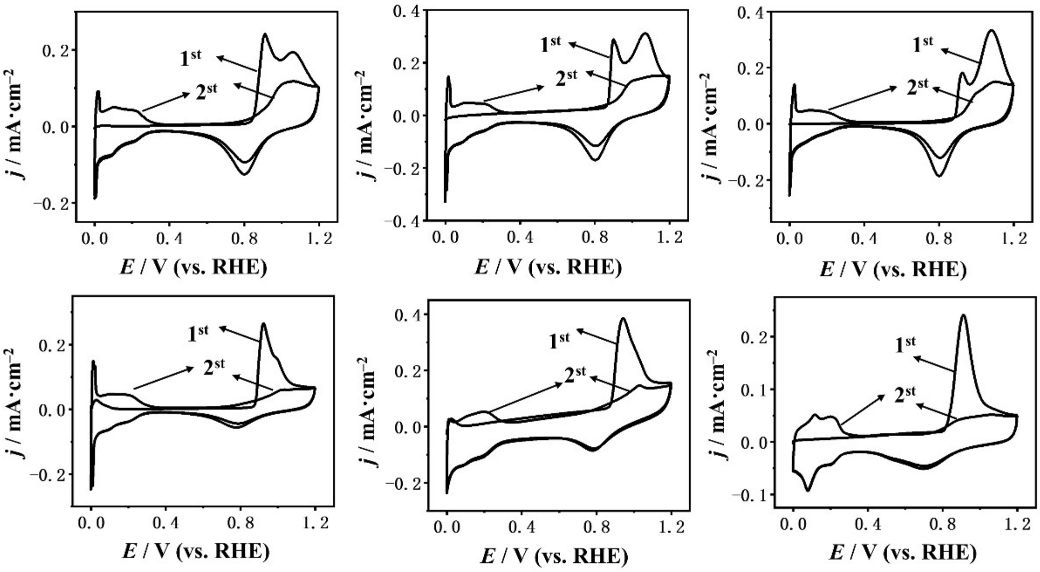

Fig. S8 CO stripping curves for 1st and 2nd cycles of different catalysts in 0.5 M H_2SO_4. Scanning rates, 50 mV s^{-1}.

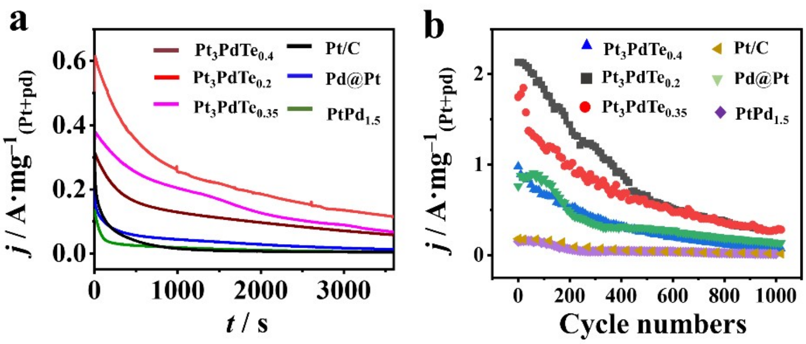

Fig. S9 Durability tests of electrocatalysts towards electrooxidations of 1 M methanol in 0.1 M $HClO_4$ according to chronoamperometry curves at 0.76 V for 3600 s (a) and peaked mass activities in the backward scans in continuous CVs at 50 mV·s^{-1} (b).

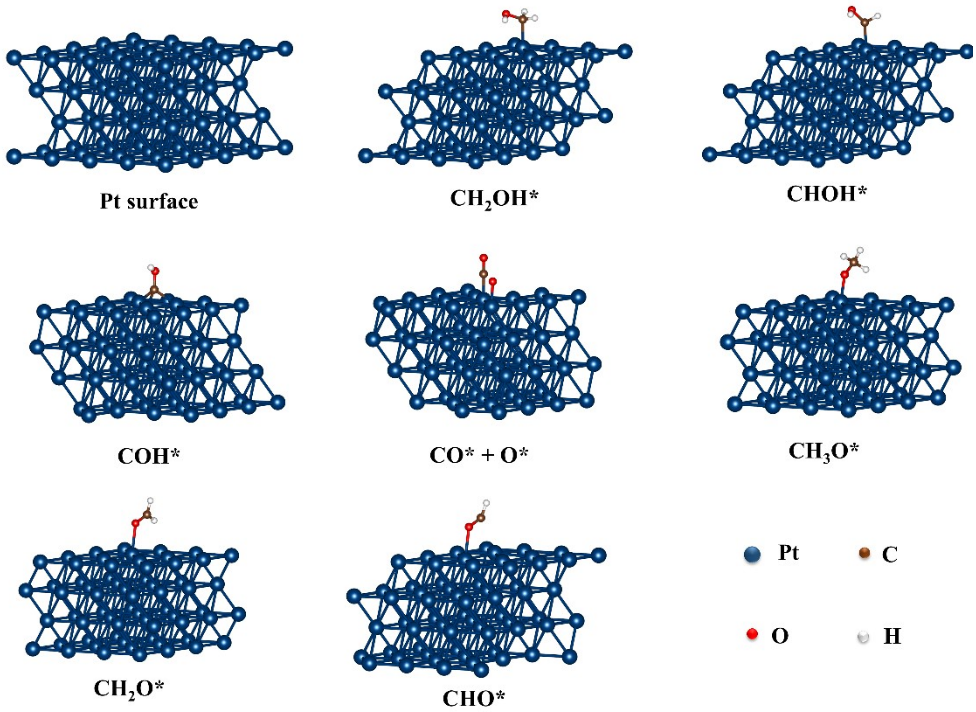

Fig. S10 Configurations of Pt and the intermediates.

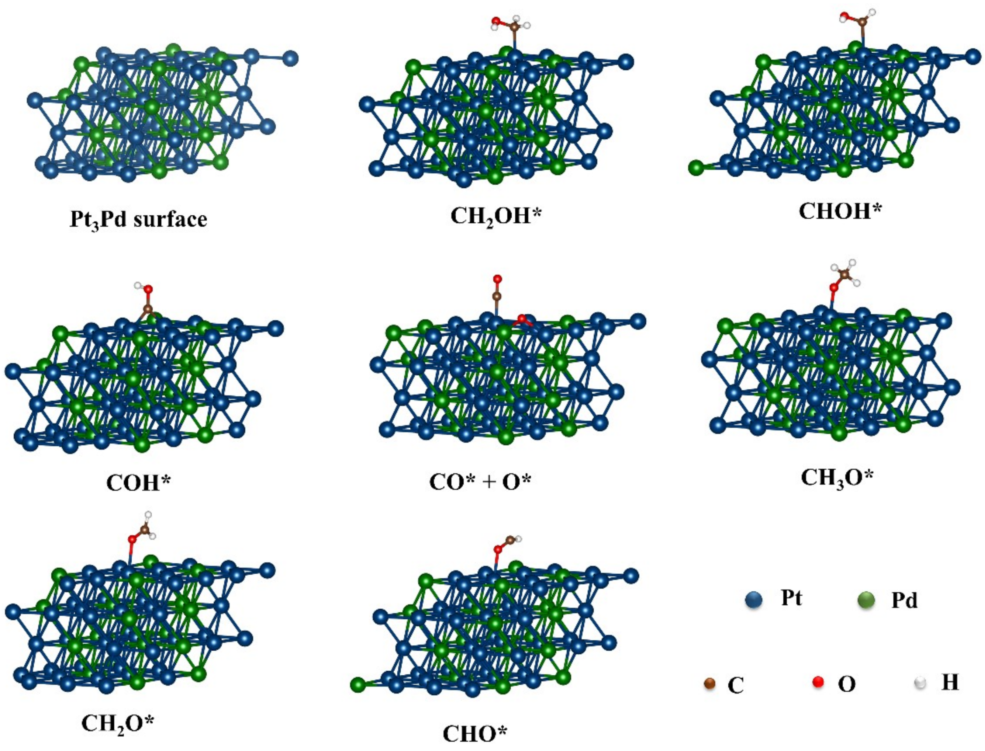

Fig. S11 Configurations of Pt_3Pd and the intermediates.

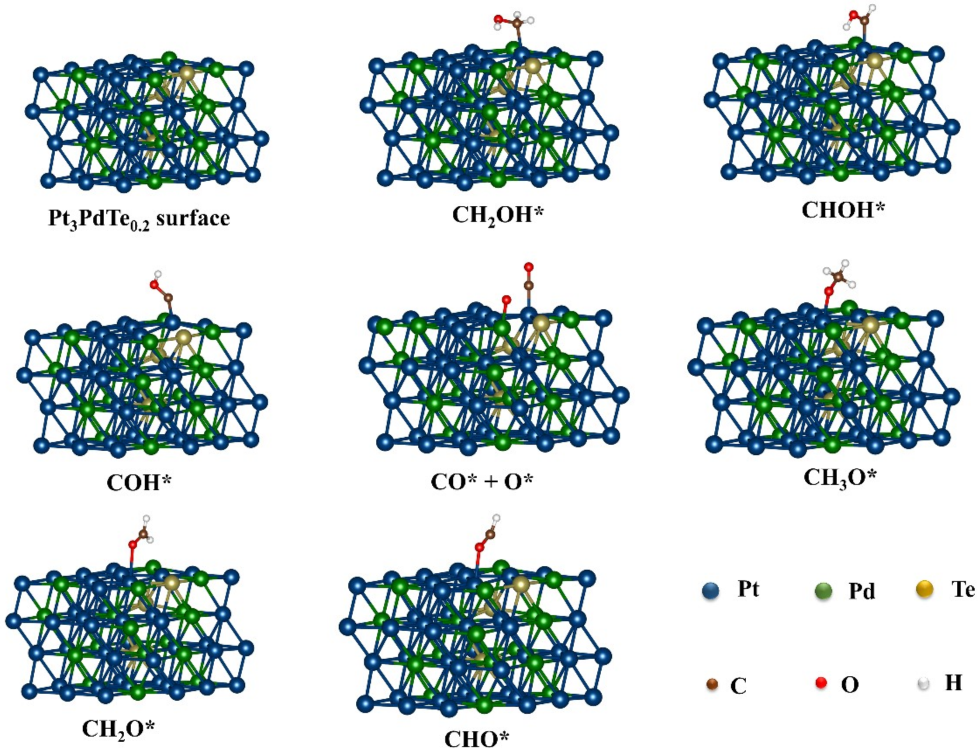

Fig. S12 Configurations of $Pt_3PdTe_{0.2}$ and the intermediates.

References

1. S. Y. Ma, H. H. Li, B. C. Hu, X. Cheng, Q. Q. Fu and S. H. Yu, *J. Am. Chem. Soc.*, 2017, **139**, 5890-5895.
2. H.-H. Li, S. Zhao, M. Gong, C.-H. Cui, D. He, H.-W. Liang, L. Wu and S.-H. Yu, *Angew. Chem. Int. Ed.*, 2013, **52**, 7472-7476.
3. Z. Wang, H. Zhang, S. Yin, S. Liu, Z. Dai, Y. Xu, X. Li, L. Wang and H. Wang, *Sustain. Energy Fuels*, 2020, **4**, 2950-2955.
4. L. Yang, G. Li, J. Ge, C. Liu, Z. Jin, G. Wang and W. Xing, *J. Mater. Chem. A*, 2018, **6**, 16798-16803.
5. Y. Hao, Y. Yang, L. Hong, J. Yuan, L. Niu and Y. Gui, *ACS Appl. Mater. Interfaces*, 2014, **6**, 21986-21994.
6. C. Shang, Y. Guo and E. Wang, *Nano Res.*, 2018, **11**, 4348-4355.
7. L. Huang, X. Zhang, Q. Wang, Y. Han, Y. Fang and S. Dong, *J. Am. Chem. Soc.*, 2018, **140**, 1142-1147.
8. L. Wang and Y. Yamauchi, *J. Am. Chem. Soc.*, 2013, **135**, 16762-16765.
9. P. Wang, Y. Zhang, R. Shi and Z. Wang, *ACS Appl. Energy Mater.*, 2019, **2**, 2515-2523.